

Supplementary Information

Primary amines protect against retinal degeneration in mouse models of retinopathies

Akiko Maeda^{1,2}, Marcin Golczak², Yu Chen², Kiichiro Okano², Hideo Kohno²,
Satomi Shiose², Kaede Ishikawa², William Harte³, Grazyna Palczewska⁴,
Tadao Maeda^{1,2}, and Krzysztof Palczewski²

¹Department of Ophthalmology and Visual Sciences, Case Western Reserve University, Cleveland, USA.

Akiko Maeda, Tadao Maeda

²Department of Pharmacology, Case Western Reserve University, Cleveland, Ohio, USA.

Akiko Maeda, Marcin Golczak, Yu Chen, Kiichiro Okano, Hideo Kohno, Satomi Shiose, Kaede Ishikawa, Tadao Maeda, Krzysztof Palczewski

³Polgenix Inc., Cleveland, Ohio 44106, USA.

Grazyna Palczewska

⁴Visum Inc.; Cleveland, Ohio 44106, USA.

William Harte

Table of contents

	Page
1. Supplementary Methods	2
2. Supplementary Results	8

Supplementary Methods

Materials. Fresh bovine eyes were obtained from a local slaughterhouse (Orrville, OH). AtRAL and atROL were purchased from Toronto Research Chemicals (TRC, Toronto, Canada). Deuterated atRAL (D6-atRAL, 96%) was obtained from Cambridge Isotope Labs (Andover, MA). The names of primary amines (A) are given in **Supplementary Table 1**. Amine A1 (Cat # 112909), A2 (390593), A3 (M-9292), A5 (P-8511), A6 (A-89855), A7 (A-74807), A8 (A-79604), A9 (F-2802), A10 (C-7670), A12 (P-4875), A14 (I-0160), A15 (L-6292), A17 (A-5605), A18 (D-9628), A19 (C-4911), and A23 (R-116) were purchased from Sigma-Aldrich (St. Louis, USA). Amine A4 (Cat # P-318830), A13R (S-491000), A16 (M-110200), and A21 (A-919960) were obtained from Toronto Research Chemicals Inc. (Toronto, Canada). Amine A11 (Cat # 08088) and A22 (09409) were bought from Fluka (Buchs, Switzerland). Custom-made A13S was ordered from Aroz technologies, LLC (Cincinnati, OH) and A20R from Ricerca (Cleveland, OH). A20S was obtained from a local drug store (CVS) based on a prescription from a Case Western Reserve University veterinarian.

Characterization of synthetic compounds. Retinylamine was synthesized and purified according to the method published by Golczak *et al.* ¹ HPLC elution (Agilent XDB-C18, 250 x 4.6, 5 μ m column, linear gradient of acetonitrile in water (0–100% acetonitrile over 20 min at a flow rate of 1.5 ml/min): 18 min. UV/Vis (ethyl acetate): λ_{\max} 326 nm. ¹H NMR (400 MHz, CDCl₃) δ (ppm) 1.00 (s, 6H), 1.45 (m, 2H), 1.58 (m, 2H), 1.68 (s, 3H), 1.87 (s, 3H), 1.91 (s, 3H), 1.99 (t, 2H, J = 5.8 Hz), 3.74 (d, 2H, J = 6.4 Hz), 5.65 (m, 1H), 6.0–6.2 (m, 3H), 6.25 (d, 1H, J = 15.2 Hz), 6.6 (dd, 1H, J = 11.4 Hz, 15.2 Hz). ¹H NMR (400 MHz, CDCl₃) δ (ppm) 1.00 (s, 6H), 1.45 (m, 2H), 1.58 (m, 2H), 1.68 (s, 3H), 1.87 (s, 3H), 1.91 (s, 3H), 1.99 (t, J = 5.8 Hz, 2H), 3.74 (d, J = 6.4 Hz, 2H), 5.65 (m, 1H), 6.0–6.2 (m, 3H), 6.25 (d, J = 15.2 Hz, 1H), 6.6 (dd, J = 11.4 Hz, 15.2 Hz, 1H).

N-retinyl-*N*-retinylidene-ethanolamine (A2E) and
10-deuterated-*N*-retinyl-*N*-retinylidene-ethanolamine: A2E and its

deuterated derivative were synthesized accordingly to the procedure described in Parish *et al.* ² and purified on a reverse phase C18 column (Agilent XDB-C18, 250 x 4.6, 5 μ m) in a linear gradient of acetonitrile in water (80 – 100% acetonitrile over 20 min at a flow rate of 1.5 ml/min). Both solvents contained 0.05% trifluoroacetic acid (TFA). HPLC elution: 9.0 min. UV/Vis (acetonitrile): λ_{\max} 336 nm and 440 nm. APCI-MS (m/z): [M]⁺ calculated for C42H58ON m/z = 592.451 and C42H48D10ON m/z = 602.591; found, 592.46 and 602.60, respectively. MS² fragmentation pattern for A2E and corresponding peaks for 10-deuterated A2E (**bold**), fragmentation energy 25 V (m/z): 576.5, **586.6**, 562.6, **572.6**, 548.5, **558.6**, 486.5, **490.5**, 468.4, **478.5**, 442.3, **452.5**, 432.4, **442.5**, 418.5, **425.5**, 404.0, **411.4**, 392.5, **399.5**, 378.2, **385.4**, 364.3.0, **368.4**, 338.3, and **342.3**.

N-retinylidene-5-methoxy-1-[4-(trifluoromethyl)phenyl]pentan-1-one

O-2-aminoethyl oxime: D6-atRAL was reacted with a 2 molar excess of (*E*)-5-methoxy-1-[4-(trifluoromethyl)phenyl]pentan-1-one *O*-2-aminoethyl oxime in ethanol. Reaction products were separated by reverse phase HPLC (Agilent Zorbax Eclipse XBD C18, 5 μ m, 4.6 x 150 mm column) with a linear gradient of acetonitrile in water (50 – 100%) at a flow rate of 1.5 ml/min over 20 min. Both solvents were supplemented with 0.05% TFA. HPLC elution: 11.5 min. UV/Vis (acetonitrile, TFA): λ_{\max} 450 nm. APCI-MS (m/z): [M]⁺ calculated for C35H47F3N2O2 m/z = 585.36 and C35H41D6F3N2O2 m/z = 591.40; found 584.42 and 591.54, respectively. MS² fragmentation pattern for the compound and its 6-deuterated derivative (**bold**), fragmentation energy 25 V (m/z): 493.4, **496.4**, 435.2, **441.4**, 395.2, **398.4**, 371.3, **374.4**, 326.3, **332.4**, 319.2, **320.3**, 310.3, **316.4**, 367.2, **273.4**, 260.2, **261.3**, 234.2, **237.3**, 218.2, and **221.3**.

*N-retinylidene-4-oxo-4-[3-(trifluoromethyl)-5,6-dihydro[1,2,4]triazolo[4,3-*a*]pyrazin-7(8*H*)-yl]-1-(2,4,5-trifluorophenyl)butan-2-amine*: Reaction

conditions and purification were identical to those described above. HPLC elution: 8.2 min. UV/Vis (acetonitrile, TFA): λ_{\max} 460 nm. APCI-MS (m/z): [M]⁺ calculated for C36H41F6N5O m/z = 673.32 and C36H35D6F6N5O m/z = 680.33; found 674.45 and 680.53, respectively. MS² fragmentation pattern

for the compound and its 6-deuterated derivative (bold) fragmentation energy 25 V (m/z): 594.3, **597.4**, 582.4, **585.4**, 550.3, **556.4**, 538.3, **544.4**, 530.4, **524.2**, 498.2, **501.3**, 484.2, **487.3**, 460.3, **463.3**, 440.4, **446.4**, 408.2, **408.2**, 391.2, **391.2**, 267.2, **273.4**, 241.2, **247.2**, 235.2, and **235.2**.

N-retinylidene-3-(aminomethyl)-5-methylhexanoic acid: Reaction conditions and purification were identical to those described above. HPLC elution: UV/Vis (acetonitrile, TFA): λ_{\max} 455 nm. APCI-MS (m/z): $[M]^+$ calculated for C₂₈H₄₃NO₂ m/z = 426.33 and C₂₈H₃₇D₆NO₂ m/z = 432.34; found 426.45 and 432.55, respectively. MS² fragmentation pattern for the compound and its 6-deuterated derivative (bold) fragmentation energy 25 V (m/z): 408.3, **414.5**, 334.3, **337.4**, 302.2, **308.4**, 284.3, **290.4**, 276.2, **282.4**, 267.2, **273.4**, 236.2, **239.3**, 212.2, **215.3**, 177.2, **180.2**, 158.2, and **158.2**.

N-retinylidene-retinylamine: Reaction conditions and purification were identical to those described above. HPLC elution: UV/Vis (acetonitrile, TFA): λ_{\max} 329 and 452 nm. APCI-MS (m/z): $[M]^+$ calculated for C₄₀H₅₇N m/z = 552.45 and C₄₀H₅₁D₆N m/z = 558.46; found 552.50 and 558.52, respectively. MS² fragmentation pattern for the compound and its 6-deuterated derivative (bold) fragmentation energy 25 V (m/z): 553.7, **556.7**, 523.6, **529.6**, 496.6, **502.6**, 460.5, **463.5**, 428.5, **434.5**, 416.5, **422.5**, 414.5, **420.5**, 402.4, **408.5**, 391.4, **394.5**, 376.5, **382.5**, 362.4, **365.4**, 348.4, **351.4**, 269.2, and **269.2**.

(R)-3-aminomethyl-5-methylhexanoic acid: $[\alpha]_D^{25} = -10.7$. ¹H NMR (400 MHz, D₂O) δ (ppm) 0.85 (dd, *J* = 4.8 Hz, 6.4 Hz, 6H), 1.18 (t, *J* = 7 Hz, 2H), 1.62 (m, 1H), 2.12 (m, 1H), 2.2 (dd, *J* = 7 Hz, 14.6 Hz, 1H), 2.28 (dd, *J* = 6.2 Hz, 14.6 Hz, 1H), 2.89 (dd, *J* = 6.4 Hz, 13.2 Hz, 1H), 2.97 (dd, *J* = 5.4 Hz, 13.2 Hz, 1H).

(S)-4-oxo-4-[3-(trifluoromethyl)-5,6-dihydro[1,2,4]triazolo[4,3-a]pyrazin-7(8H)-yl]-1-(2,4,5-trifluorophenyl)butan-2-amine: $[\alpha]_D^{25} = +17.4$. ¹H NMR (400 MHz, D₂O) δ (ppm) 2.8–3.1 (m, 4H), 4.0 (m, 3H), 4.26 (m, 1H), 4.31 (m, 1H), 4.97 (m, 2H), 7.13 (m, 1H), 7.28 (m, 1H).

Formation of A2E. A two molar excess of atRAL mixed with either ethanolamine or a test amine compound was stirred in ethanol in the presence of acetic acid in a sealed vial at room temperature for 3 days in the dark ². To purify the reaction products, crude reaction mixtures were injected onto a reverse phase C18 column (Phenomenex, 250 x 4.6, 5 μ m) and retinoids were separated by a linear acetonitrile–water gradient with 0.05% TFA (80 – 100% acetonitrile over 20 min at a flow rate of 1.5 ml/min). The presence of A2E was detected based on its characteristic UV/Vis absorbance spectrum. Fractions with peaks corresponding to products of interest were collected and analyzed by tandem mass spectrometry. Isotopically labeled A2E used for MS quantification was prepared as described above.

Mouse eye A2E purification and analysis. Two enucleated mouse eyes were homogenized in 1 ml of prechilled –20°C acetonitrile with a kinematic Polytron homogenizer (PT 1200). The resulting sample was then homogenized in a glass–glass homogenizer, extracted twice with 1 ml of acetonitrile and centrifuged at 13,000g for 2 min. The supernatant was collected, transferred to a glass test tube, and dried down in a SpeedVac. Prior to HPLC separation, the sample was dissolved in 0.2 ml of acetonitrile supplemented with 0.1% TFA and filtered through a Teflon syringe filter (National Scientific Company, Rockwood, TN). Extracted retinoids were separated on a C18 reverse–phase HPLC column (Agilent Zorbax Eclipse XBD C18, 5 μ m, 4.6 x 150 mm) with a linear gradient of acetonitrile in water (80 – 100%) and 0.1% TFA at a flow rate of 1.5 ml/min for 30 min. Elution of A2E was monitored at 435 nm.

Mass spectrometry and quantification of A2E. After mouse eye extracts were loaded on a C18 reverse–phase HPLC column (Agilent Zorbax Eclipse XBD C18, 5 μ m, 4.6 x 150 mm), a linear gradient of acetonitrile in water (80 – 100%) with 0.05% TFA run over 30 min at a flow rate of 1.5 ml/min was used to elute retinoids. Eluents were directed into a LXQ mass spectrometer through an APCI source. To achieve optimal sensitivity, the instrument was

tuned first with synthetic A2E or an A2E-like standard. Deuterated A2E synthesized from commercially available D6-atRAL was used as an internal standard for quantification. Known amounts of an appropriate deuterated standard (10 – 60 pmol) were added to each sample prior to homogenization. The ratio between signals corresponding to the deuterated and endogenous retinoids was used for precise quantification of A2E.

Formation of a Schiff base between retinal and selected amines. A stock solution of atRAL was made freshly in ethanol, and the final concentration of retinal was determined spectrophotometrically at 380 nm ($\epsilon = 42,880$). Schiff base formation was initiated by addition of the retinal stock to a solution containing 2 molar excess of the tested primary amine. Reaction mixtures were incubated for 1 h at room temperature. Schiff base formation was monitored by changes in absorbance at 380 and 450 nm (510 nm for aromatic amines) corresponding to free retinal and the protonated Schiff base, respectively. Reaction products were separated by reverse phase HPLC (Agilent Zorbax Eclipse XBD C18, 5 μ m, 4.6 x 150 mm column) with a linear gradient of acetonitrile in water (50 – 100%) at a flow rate of 1.5 ml/min over 20 min. Both solvents were supplemented with 0.05% TFA to provide acidic conditions for detection of retinyl imines at 450 nm. Fractions with peaks containing imines were collected and their purity was checked by tandem mass spectrometry. The same methodology was used to prepare isotopically-labeled retinylidene Schiff base standards from D6-atRAL.

Quantification of 11-*cis*-retinal. All experimental procedures related to extraction, derivatization, and separation of retinoids from dissected mouse eyes were performed as described previously³. Reactions involving retinoids were carried out under dim red light. Retinoids were separated by normal phase HPLC (Ultrasphere-Si, 4.6 μ 250 mm, Beckman, Fullerton, CA) with 10% ethyl acetate and 90% hexane at a flow rate of 1.4 ml/min with detection at 325 nm using an HP1100 HPLC with a diode array detector and HP Chemstation A.03.03 software. The percent of 11-*cis*-retinal remaining after

illumination was calculated as follows: (data – vehicle treated and light expose / vehicle treated and not light exposed – vehicle treated and light exposed) x 100.

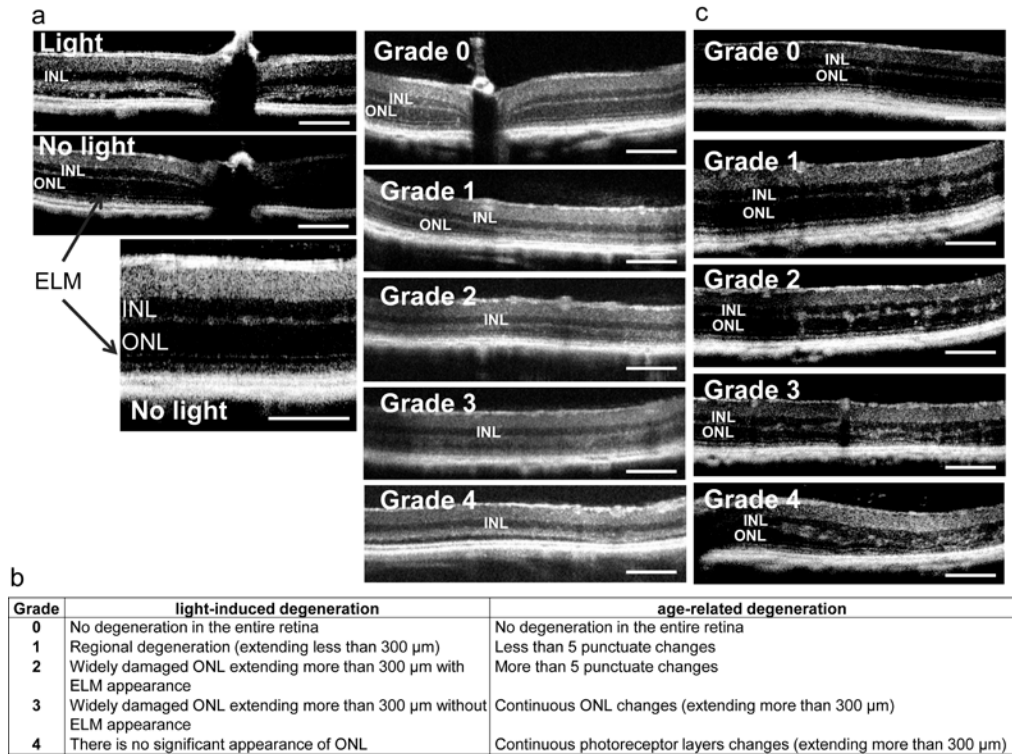
Histology. Histological and immunohistochemical analyses employed established procedures⁴. 2-(4-amidinophenyl)-1H-indole-6-carboxamide (DAPI) was purchased from Invitrogen (Carlsbad, CA). Eyecups for histology were fixed in 2% glutaraldehyde/4% paraformaldehyde and processed for embedding in Epon. One μm sections were cut and stained with toluidine blue⁴.

References

- 1 Golczak, M., Kuksa, V., Maeda, T., Moise, A. R. & Palczewski, K. Positively charged retinoids are potent and selective inhibitors of the trans-cis isomerization in the retinoid (visual) cycle. *Proc Natl Acad Sci U S A* **102**, 8162–8167, (2005).
- 2 Parish, C. A., Hashimoto, M., Nakanishi, K., Dillon, J. & Sparrow, J. Isolation and one-step preparation of A2E and iso-A2E, fluorophores from human retinal pigment epithelium. *Proc Natl Acad Sci U S A* **95**, 14609–14613, (1998).
- 3 Van Hooser, J. P. *et al.* Rapid restoration of visual pigment and function with oral retinoid in a mouse model of childhood blindness. *Proc Natl Acad Sci U S A* **97**, 8623–8628, (2000).
- 4 Maeda, A. *et al.* Role of photoreceptor-specific retinol dehydrogenase in the retinoid cycle in vivo. *J Biol Chem* **280**, 18822–18832, (2005).

Supplementary Results

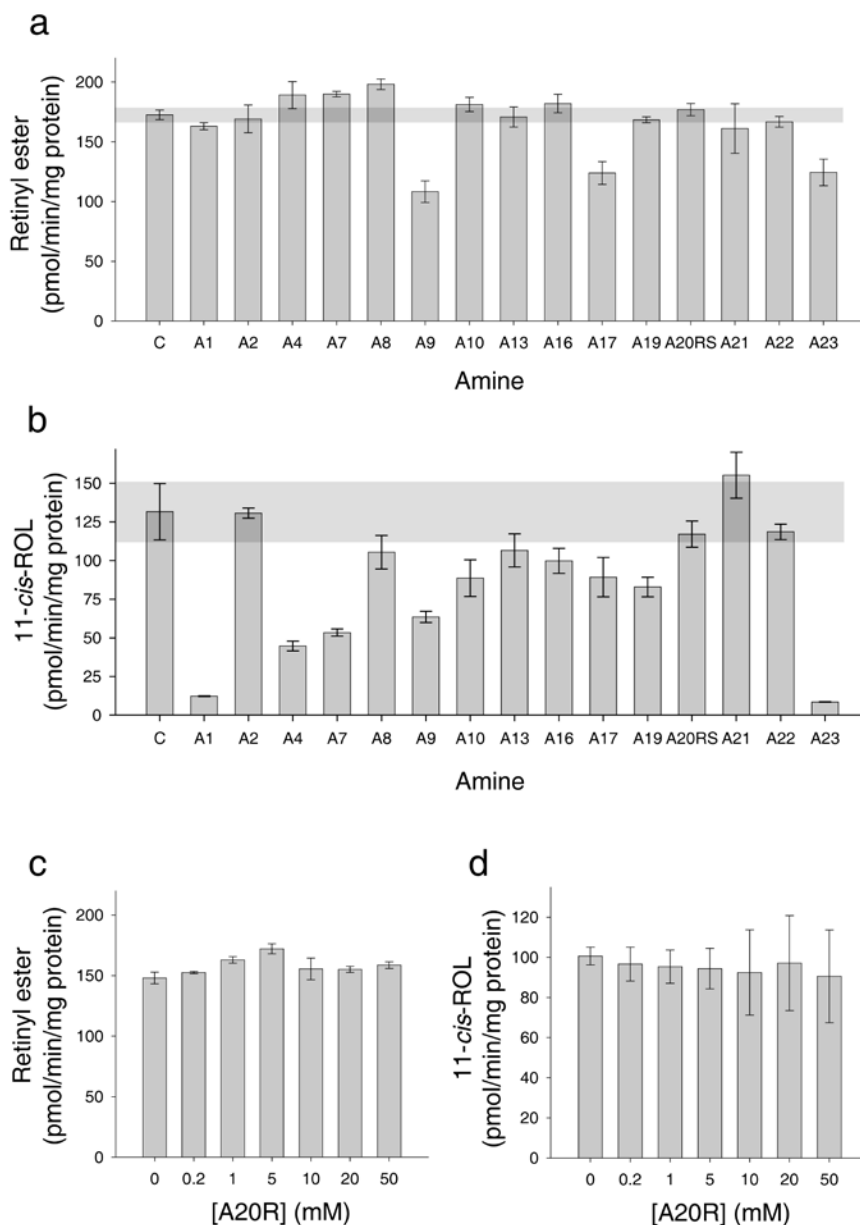
Supplementary Item & Number	Title or Caption
Supplementary Figure 1	<i>In vivo</i> imaging of mouse retinas by OCT: grading retinopathy to assess the efficacy of primary amine drug pretreatment in protecting against bright light-induced and age-related retinal degeneration.
Supplementary Figure 2	Effects of primary amines on LRAT and retinoid isomerization activities displayed by bovine RPE microsomes.
Supplementary Figure 3	Effect of primary amines on 11- <i>cis</i> -retinal regeneration.
Supplementary Figure 4	Time-dependent effect of primary amine A20R on dark adaptation and light-induced degeneration after bright light exposure.
Supplementary Figure 5	Effects of primary amine A22 Schiff base formation on atRAL metabolism and cytotoxicity <i>in vitro</i> .
Supplementary Figure 6	Quantification of retinylidenes in mouse eye after administration of amine A20.
Supplementary Figure 7	The spectra of condensation products between all- <i>trans</i> -retinal and 3-aminomethyl-5-methylhexanoic acid.
Supplementary Figure 8	An example of A2E quantification in mouse retina.
Supplementary Figure 9	Effects of treatment with primary amine drugs on age-related retinal degeneration in <i>Abca4</i> ^{-/-} <i>Rdh8</i> ^{-/-} mice.
Supplementary Figure 10	Effects of A20RS on retinal degeneration in rhodopsin-palmitoylation deficient and <i>Rdh12</i> ^{-/-} mice.
Supplementary Table 1	Primary amines tested for protection against light-dependant retinal degeneration in <i>Abca4</i> ^{-/-} <i>Rdh8</i> ^{-/-} mice.
Supplementary Table 2	Distribution of SLO gray values after primary amine treatment of <i>Abca4</i> ^{-/-} <i>Rdh8</i> ^{-/-} mice for 3 months.



Supplementary Figure 1. *In vivo* imaging of mouse retinas by OCT: grading retinopathy to assess the efficacy of primary amine drug pretreatment in protecting against bright light-induced and age-related retinal degeneration.

(a, b) Grading for bright light-induced retinal degeneration. **Left column:** *In vivo* retinal images obtained by OCT 7 days after 4-week-old *Abca4^{-/-}Rdh8^{-/-}* mice were exposed to 10,000 lux light for 30 min. Light-illuminated animals displayed severe retinal degeneration (upper panel). The external limiting membrane (ELM) is shown in low and higher magnification of an *Abca4^{-/-}Rdh8^{-/-}* mouse non-illuminated retina (arrows in middle and lower panel). **Right column:** OCT analyses were performed 7 days after 4-week-old *Abca4^{-/-}Rdh8^{-/-}* mice pretreated with a test drug were exposed to 10,000 lux light for 30 min. The severity of retinal degeneration shown is graded from 0 to 4. (b, c) Grading by OCT to assess the severity of

age-related retinal degeneration. *In vivo* retinal images were obtained by OCT after test drug gavage of *Abca4*^{-/-}*Rdh8*^{-/-} mice for 3 months starting at 1 month of age. *Abca4*^{-/-}*Rdh8*^{-/-} mice displayed age-related retinal degeneration, initially observed at 1–2 months of age. The severity of retinal degeneration was graded from 0 to 4. ONL, outer nuclear layer; INL, inner nuclear layer. Bars: 100 μm. After degeneration of the retina induced by light, it took 7 days before all cells were cleared. However, changes in OCT images were detected in the ONL region starting 1 day after light exposure. But only a few apoptotic cells were detected 7 days after light exposure. Thus, to quantify retinal degeneration, 7 days was chosen to allow virtually complete clearance of dead cells¹.

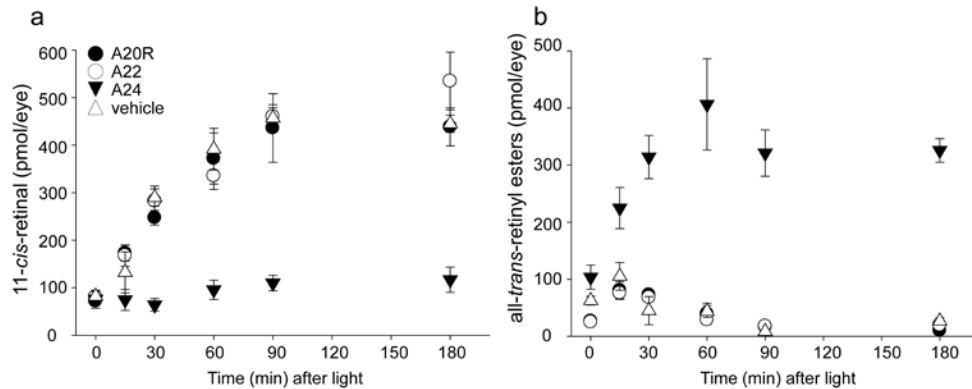


Supplementary Figure 2. Effects of primary amines on LRAT and retinoid isomerization activities displayed by bovine RPE microsomes.

(a) Screening of primary amines for inhibition of LRAT activity in RPE microsomes. Enzymatic assays were carried out with 1 mM 1,2-diheptanoyl-sn-glycero-3-phosphocholine (donor of heptanoyl group),

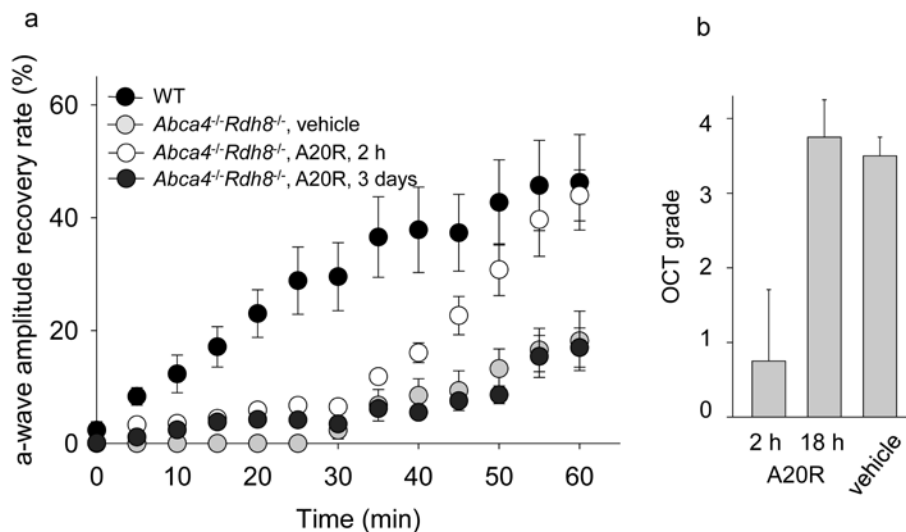
10 μ M atROL and 1 mM of tested primary amines in 25 mM Tris/HCl buffer, pH 8.0. To measure the effect of primary amines on initial rates of retinyl ester formation, reaction mixtures were incubated for 2 min at room temperature and then quenched with methanol. Retinoids were extracted with hexane and retinyl ester production was quantified by normal phase HPLC.

(b) Effects of selected primary amines on RPE65-dependent retinoid isomerization. Bovine RPE microsomes resuspended in 0.2 ml of 50 mM Bis-Tris propane buffer, pH 7.5, 1 % BSA, and 1 mM ATP were preincubated with 1 mM of tested primary amines for 10 min at room temperature. Retinoid isomerization was initiated by adding atROL (10 μ M) followed by CRALBP. Reaction mixtures were incubated at 30°C for 10 min, quenched with 0.3 ml of methanol and extracted with hexane. Retinoid composition then was determined by normal phase HPLC. Panels **c** and **d** represent LRAT and RPE65 enzymatic activity, respectively, in the presence of increasing concentrations of A20R. All data represent average values obtained from two independent experiments performed in triplicate (error bars indicate S.D.).



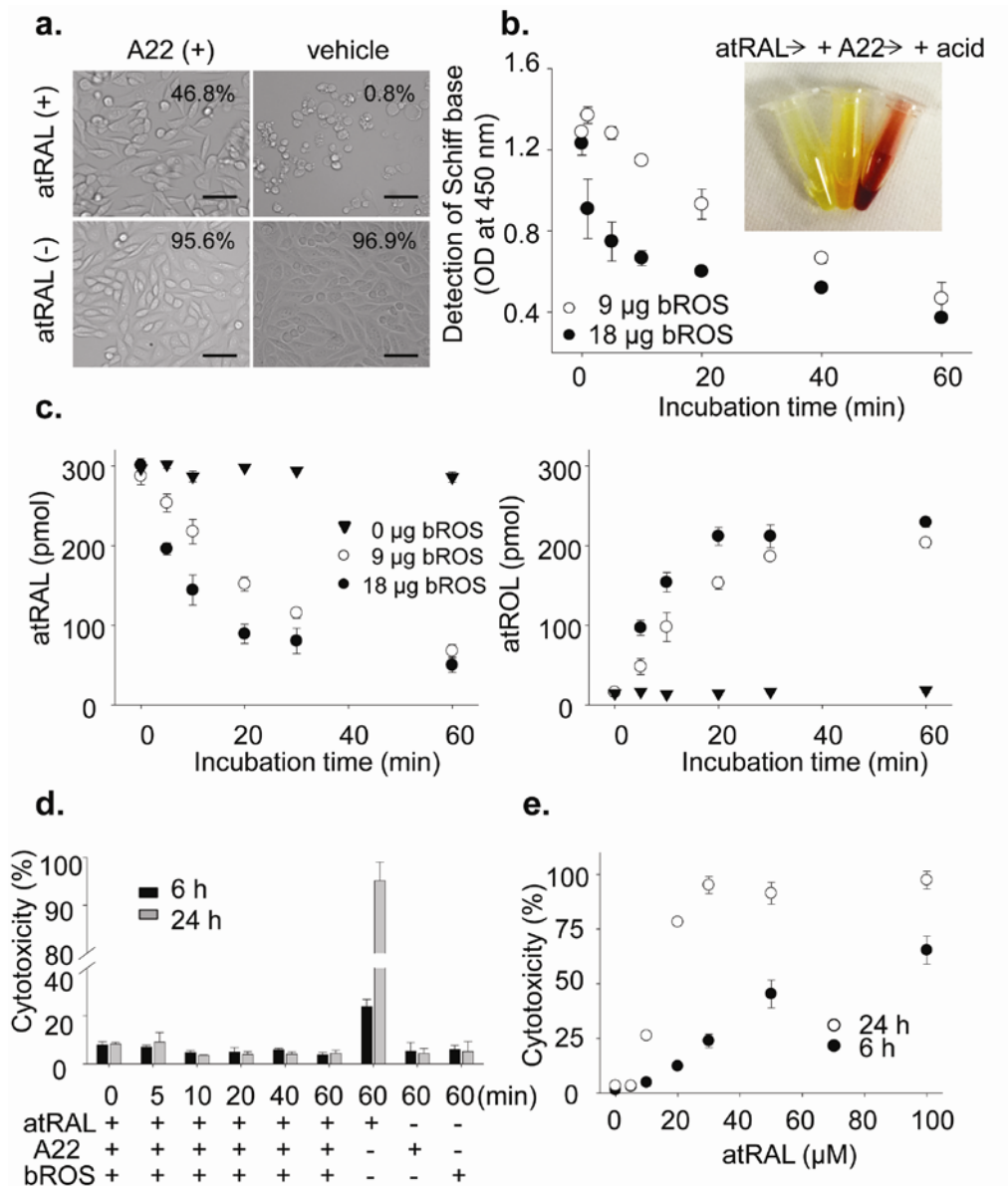
Supplementary Figure 3. Effect of primary amines on 11-*cis*-retinal regeneration.

Regeneration of 11-*cis*-retinal (**a**) and kinetics of all-*trans*-retinyl ester formation (**b**) were examined after ~90% of rhodopsin bleached by illumination at 10,000 lux for 3 min. Four-week-old *Abca4*^{-/-}*Rdh8*^{-/-} mice kept in the dark for 48 h were administered A20R, A22 or A24 (2 mg/mouse) by oral gavage 2 h (A20R and A22) or 16 h (A24) before the light exposure. Mice then were returned to the dark for indicated time when final retinoid analyses shown were performed. Retinoids were extracted with hexane and amounts of 11-*cis*-retinal and all-*trans*-retinyl esters were quantified by normal phase HPLC. As expected A24 blocked conversion of retinyl esters (which over-accumulated) to 11-*cis*-retinal, but other primary amines did not interfere with visual cycle. Bars indicate S.D. of the means (n = 6).



Supplementary Figure 4. Time-dependent effect of primary amine A20R on dark adaptation and light-induced degeneration after bright light exposure.

(a) Dark-adapted 4-week-old *Abca4*^{-/-}*Rdh8*^{-/-} mice were pretreated with A20R (2 mg/mouse) 2 h before ERG examination. Mice were bleached with intense constant illumination (500 cd·m⁻²) for 3 min and the recovery of a-wave amplitudes was monitored with single-flash ERG (-0.2 cd·s·m⁻²) for 60 min. The recovery rate was significantly attenuated in *Abca4*^{-/-}*Rdh8*^{-/-} mice (p<0.01 at 5, 20 and 60 min after bleaching) compared with WT mice. A20R-pretreated *Abca4*^{-/-}*Rdh8*^{-/-} mice showed improved recovery 2 h after drug treatment but this improvement disappeared 3 days after treatment cessation (half-life of A20 in mouse serum was 5–6 h). Bars indicate S.D. of the means (n = 6). (b) A20R was administered to 4-week-old *Abca4*^{-/-}*Rdh8*^{-/-} mice (2 mg/mouse), and mice were illuminated with 10,000 lux light for 30 min, 2 h or 18 h after drug treatment. SD-OCT was performed 7 days after light exposure. Retinal structure was significantly preserved when mice were treated with A20R 2 h before the light exposure, but severe degeneration was observed if A20R was largely eliminated as was the case when mice were treated with this primary amine 18 h before light exposure. Bars indicate S.D. of the means (n = 4).

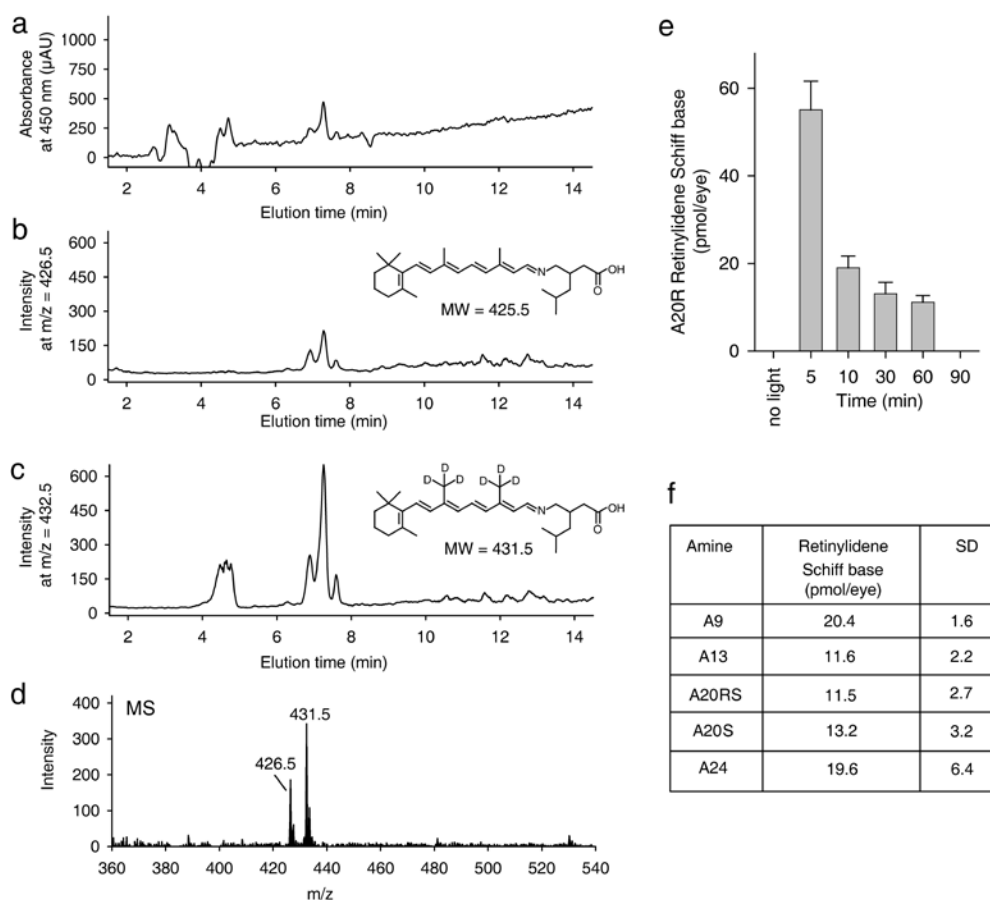


Supplementary Figure 5. Effects of primary amine A22 Schiff base formation on atRAL metabolism and cytotoxicity *in vitro*.

(a) Effects of primary amines on cell viability were examined after co-incubation with atRAL. ARPE19 cells in 24 well plates (2×10^5 cells/well) were incubated with atRAL (30 μM) and primary amine drug A22 (300 μM)

was added 10 min after co-incubation with atRAL. Images of ARPE19 cells were obtained 16 h after co-incubation with atRAL and A22 at 37°C, and the viability of cells in triplicate samples was determined with a MTT assay kit (Invitrogen). The percentage of viable cells was calculated as [(test sample – lysis control) / (saline control – lysis control)] x 100, as indicated in each image. A22 prevented ARPE19 cell death. Bar indicates 100 µm. **(b)** The kinetics of Schiff base reduction in the presence of RDH was examined by a colorimetric assay. The reaction mixture (150 µl) contained n-dodecyl-β-maltoside (1 mM), NADPH (1 mM), A22 (300 µM), and atRAL (300 µM) in 10 mM phosphate buffer (pH 7.0), and the reaction was initiated with either 9 or 18 µg of purified bovine ROS (bROS) to reduce atRAL to atROL. Reaction mixtures were incubated at 37°C for various periods, and then terminated with 10 µl of acetic acid to produce the protonated Schiff base from atRAL and A22. The color change of the atRAL and A22 mixture is shown (**inset**). The vial on the **left** containing 300 µM atRAL is light yellow. After addition of 300 µM of A22, this color changed to orange (**middle**). Addition of acetic acid produced a dark red color (**right**) due to production of the protonated Schiff base. Thus, amounts of the Schiff base was monitored at 450 – 500 nm. Bars indicate S.D. of the means (n = 3). **(c)** RDH activity of bovine rod outer segments (bROS) was examined by monitoring reduction of atRAL (**left**) and concomitant production of atROL (**right**). The reaction mixture (100 µl) contained n-dodecyl-β-maltoside (1 mM), 50 µM of atRAL, and NADPH (1 mM), and then 9 or 18 µg of bovine ROS was added to initiate the reaction. The mixture was incubated at 37°C for indicated periods, and then the reaction was terminated with 100 µl of methanol and the mixture was extracted with 500 µl of hexane. The hexane (100 µl) solution was analyzed by HPLC by using 10% ethyl acetate in hexane to assess the production of the corresponding retinoid. Rates of the Schiff base disappearance (**b**) and enzymatic reduction of atRAL (**c**) were similar. Bars indicate S.D. of the means (n = 3). **(d)** Effects of Schiff base and RDH on the cytotoxicity caused by atRAL were investigated with a lactate dehydrogenase (LDH) activity assay. ARPE19 cells were cultured in 96 well plates (2 x 10⁴ cells/90 µl/well)

and 10 μ l of reaction mixture containing atRAL, primary amine drug A22, and 18 μ g of bROS (prepared by the procedure for the Schiff base assay described in (b) but without acetic acid) was added to the medium 16 h after plating the cells. Final concentrations of atRAL and A22 before incubation were 30 μ M. Activity of LDH released from dead cells was measured with an LDH assay kit from BioVision (Mountain View, CA) after incubation at 37°C for 6 or 24 h. The percentage of cytotoxicity was calculated as [(test sample – cell negative control) / (lysis control – cell negative control)] x 100. Schiff base formation decreased the cytotoxicity of all-*trans*-retinal at earlier time points, and reduced concentrations of atRAL due to RDH activity contributed to the weaker cytotoxicity observed at the later time. Reversible Schiff base formation prevented atRAL-induced cytotoxicity. Bars indicate S.D. of the means (n = 3). (e) Cytotoxicity caused by atRAL was investigated with a lactate dehydrogenase (LDH) activity assay as described in (d). The cytotoxicity of atRAL was both time- and a dose-dependent. Bars indicate S.D. of the means (n = 3).

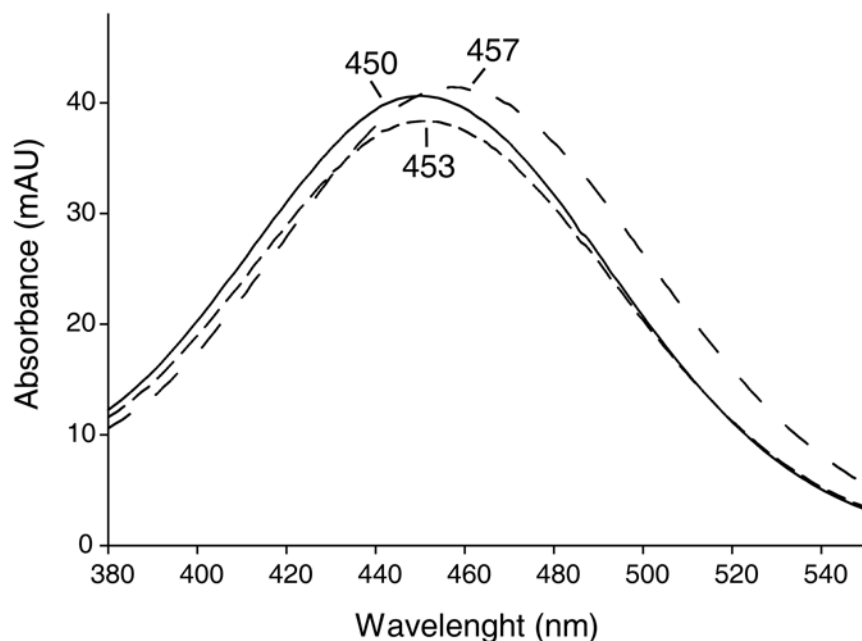


Supplementary Figure 6. Quantification of retinylidenes in mouse eye after administration of amine A20.

Four-week-old *Abca4*^{-/-}*Rdh8*^{-/-} mice kept in the dark for 48 h were administered primary amines (2 mg/mouse) by oral gavage 2 h before the light exposure. After 10,000 lux light exposure, eyes were collected and homogenized as described in Methods. Next, the mouse eye homogenate was spiked with 25 pmol of deuterated synthetic retinylidene Schiff base standard derived from amine A20RS. MS analysis of the homogenate's organic extract indicated the presence of two ions, one corresponding to the isotope-labeled standard ($m/z = 432.5$ [MH]⁺) and the other, the product of retinal condensation with amine A20RS ($m/z = 426.5$ [MH]⁺). Ratios between peak areas corresponding to these two ions served to precisely quantify the

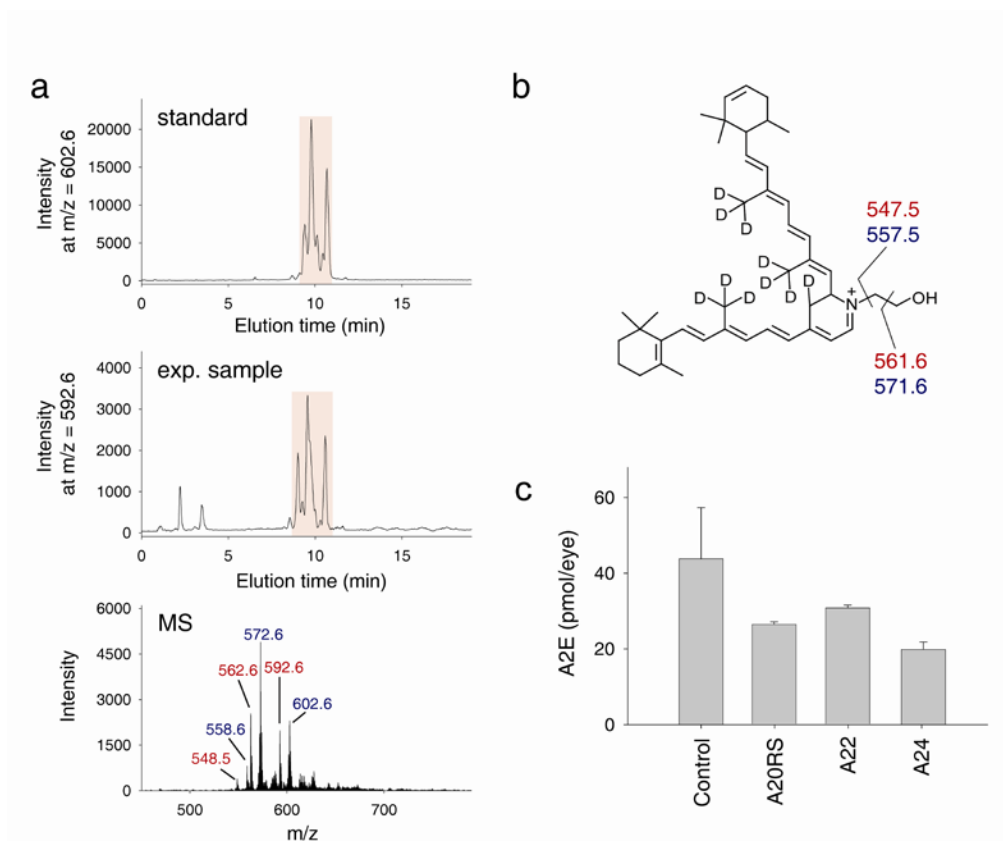
amounts of retinyl Schiff base in the examined samples. The amount of detectible Schiff base declined with time. The highest amount, reaching ~55 pmol/eye, was observed within a few minutes after light exposure. The total amount of retinal in dark-adapted mouse eye is in range of 500 pmol/eye and a 70% rhodopsin bleach liberated about 350 pmol of atRAL under our experimental conditions. Because the retinoid cycle was not affected by administration of the tested primary amines (**Supplementary Fig. 2** and **Supplementary Fig. 3a**), most atRAL was efficiently cleared by enzymatic machinery (primary reduction to retinol by RDHs). However, the fraction of free all-*trans*-retinal that cannot be processed rapidly and persists in the retina represents a critical risk factor for retinal degeneration^{1,2}. Our therapeutic approach targeted this pool of total retinals because only the excess of liberated atRAL that cannot be efficiently cleared reacts with primary amines and can be temporarily trapped in form of a Schiff base. Our experimental data suggest that elimination of 10% to 15% of total liberated atRAL (several pmol) is sufficient to lower the free retinal concentration below a cytotoxic level. To demonstrate that retinyl Schiff bases formed with selected primary amines are stable long enough to allow the enzymatic system to dispose of excess atRAL upon light exposure, we quantified these conjugates 1 h after light exposure. **(a)** Chromatogram developed to show absorbance at 450 nm. The three peaks seen in the chromatograms represent geometric isomers of *N*-retinyl-3-(aminomethyl)-5-methylhexanoic acid. At room temperature the retinoid moiety of the compound occurs in three isomers of atRAL followed by 13-*cis*-retinal and 9-*cis*-retinal. All isomers share the same molecular mass; however, their UV/Vis spectra differ slightly as expected for these isomers. Panels **(b)** and **(c)** represent extracted ion chromatograms for the internal and labeled synthetic retinyl imines, respectively. **(d)** Averaged MS signal collected between 6.6 and 7.6 min of elution time. **(e)** Quantification of A20RS retinylidene Schiff base present in the eye of treated *Abca4*^{-/-}*Rdh8*^{-/-} mice reveals a gradual decline of the conjugate over period of 90 min after light exposure at 10,000 lux for 5 min. Bars indicate S.D. of the means (n =

6). (f) Summary of retinylidene quantification for selected primary amines 1 h after light illumination at 10,000 lux for 15 min. Bars indicate S.D. of the means (n = 6).



Supplementary Figure 7. The spectra of condensation products between all-*trans*-retinal and 3-aminomethyl-5-methylhexanoic acid.

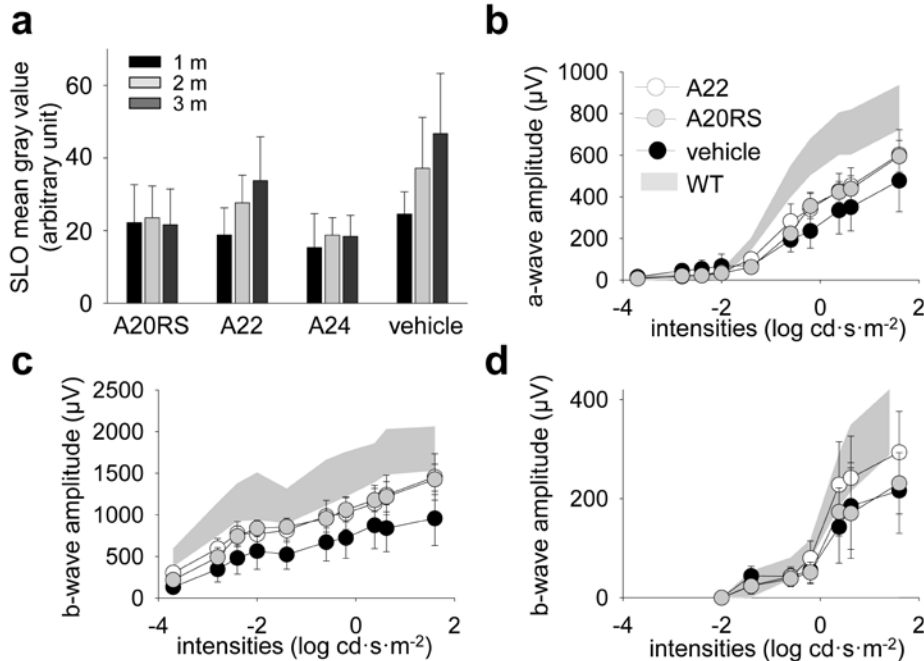
Three peaks seen in the chromatograms represent geometric isomers of *N*-retinyl-3-(aminomethyl)-5-methylhexanoic acid. The retinoid moiety of this compound can adopt several conformations. The most dominant is all-*trans* followed 13- and 9-*cis*-isomer. All isomers share the same molecular mass; however, their UV/Vis spectra differ slightly. Spontaneous isomerization of retinoids occurs upon light or thermal (room temperature) exposure.



Supplementary Figure 8. An example of A2E quantification in mouse retina.

Mouse eyes collected after long-term daily administration of amine A20RS (2 mg/mouse) for 3 months were homogenized in the presence of 60 pmol of isotopically labeled A2E. Retinoids were extracted and separated by HPLC as described in Methods. Panel (a) illustrates A2E quantification where extracted ion chromatogram for deuterated standards is shown in the **top row**. Note that the 6 deuterium atoms in the labeled atRAL used as a substrate for this biosynthesis led to incorporation of 10 deuterium atoms in the final products ($m/z = 602.6$ $[MH]^+$). **Middle row** panel represents a single ion chromatogram of retinoids extracted from mouse eyes. MS signals recorded at the elution time corresponding to the compounds of interest (9 – 10.5 min) are shown at the **bottom row**. The series of peaks corresponding to labeled internal standard and endogenous compounds are colored in blue and red, respectively. The A2E ion tends to break down under chemical

ionization conditions resulting in ions at 562.6 (loss of CH_2OH) and 548.6 (loss of $\text{C}_2\text{H}_4\text{OH}$). The fragmentation pattern and position of deuterium atoms within the A2E standard are illustrated in panel (b). (c) Summary of A2E quantification after administration of primary amine drugs is presented. Bars indicate S.D. of the means ($n = 6$).



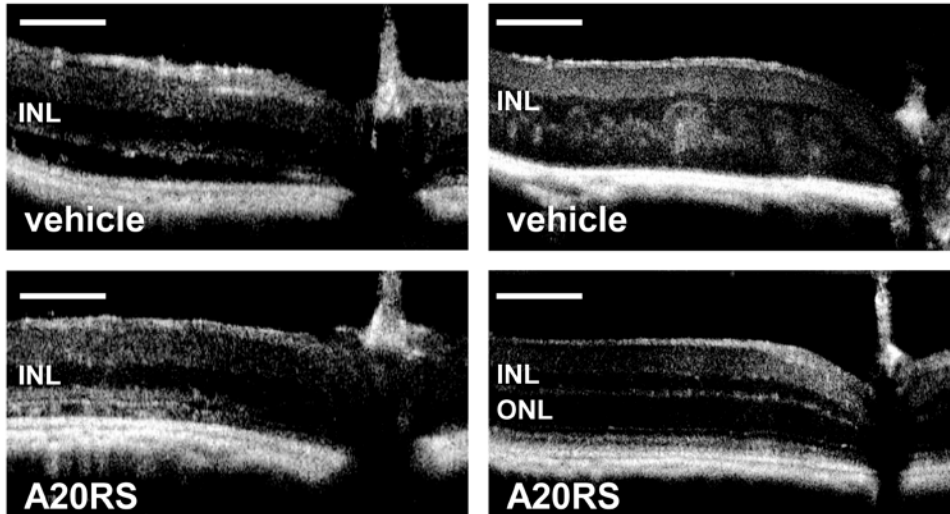
Supplementary Figure 9. Effects of treatment with primary amine drugs on age-related retinal degeneration in *Abca4*^{-/-}*Rdh8*^{-/-} mice.

Abca4^{-/-}*Rdh8*^{-/-} mice were gavaged daily with either A20RS (2 mg/mouse) or A22 (2 mg/mouse) and weekly with A24 (2 mg/mouse) for 3 months beginning at 1 month of age. (a) Intensity of fundus autofluorescence in retinas of A20RS-, A22-, A24- and vehicle-treated *Abca4*^{-/-}*Rdh8*^{-/-} mice was measured 1, 2 and 3 months after treatment; autofluorescent SLO was set at 100 sensitivity. SLO mean gray values shown were calculated by Heidelberg's SLO software. Error bars indicate S.D. of the means (n = 15 for A20RS, 15 for A22, 10 for A24 and 22 for vehicle). The intensity of autofluorescence in retinas of A20RS-, A22-, and A24-treated *Abca4*^{-/-}*Rdh8*^{-/-} mice was significantly less than that of vehicle-treated animals. (b-d) Full field ERG responses were recorded in 4-month-old *Abca4*^{-/-}*Rdh8*^{-/-} mice gavaged with A20RS, A22 or vehicle for 3 months. Responses were recorded under scotopic (a-wave, b, and b-wave, c) or photopic (d) conditions. Amplitudes of WT mice are indicated in gray. Bars indicate S.D. of the means (n = 3).

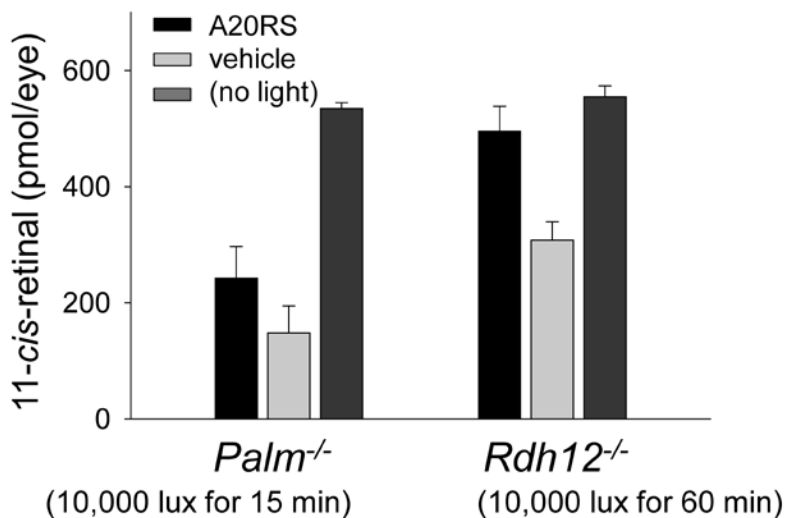
a

Palm^{-/-}: 10,000 lux for 15 min

Rdh12^{-/-}: 10,000 lux for 60 min



b

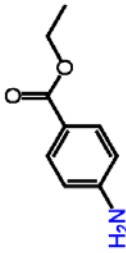
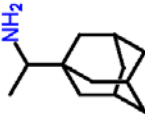


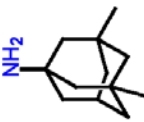
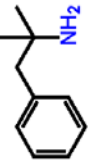

Supplementary Figure 10. Effects of A20RS on retinal degeneration in rhodopsin-palmitoylation deficient and *Rdh12*^{-/-} mice.

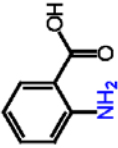
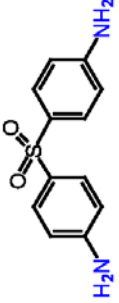
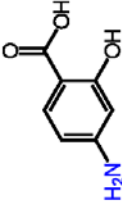
Rhodopsin-palmitoylation deficient (*Palm*^{-/-}) and *Rdh12*^{-/-} mice at 6 weeks of age were orally gavaged with a 2 mg dose of A20RS 2 h before exposure to light at 10,000 lux (15 min for *Palm*^{-/-} mice; 60 min for *Rdh12*^{-/-} mice). (a) *In*

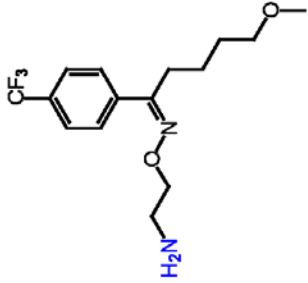
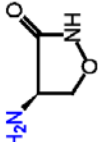
vivo imaging by OCT was performed 7 days after light exposure. Light-illuminated *Palm*^{-/-} mice showed severe retinal degeneration (grade 4 as in **Supplementary Fig. 1**), but A20RS-treated *Palm*^{-/-} mice displayed milder Grade 2 degeneration. Light-induced degeneration in *Rdh12*^{-/-} mice was completely prevented by pre-treatment with A20RS. Bars: 100 μm. **(b)** Amounts of 11-*cis*-retinal reflecting photoreceptor number were quantified by HPLC 7 days after bright light exposure. A20RS partially prevented light-induced retinal degeneration in *Palm*^{-/-} mice, but had a more marked protective effect in *Rdh12*^{-/-} mice. Error bars indicate S.D. of the means (n = 3). ONL, outer nuclear layer; INL, inner nuclear layer.

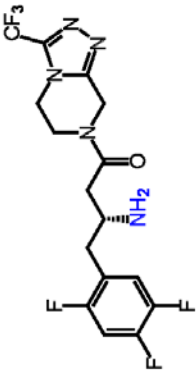
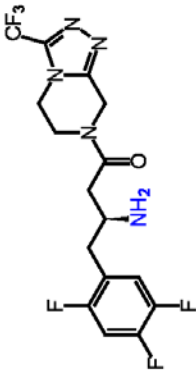
Supplementary Table 1. Primary amines tested for protection against light-dependent retinal degeneration in *Abca4*^{-/-} *Rdh8*^{-/-} mice.¹

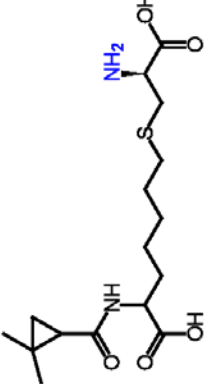
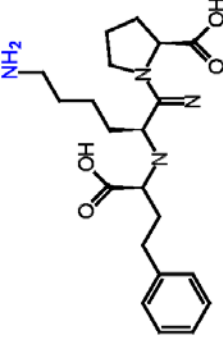
No and name	Structure and IUPAC systematic name	Indication(s)	Dose (mg/kg) and (mg per mouse)	OCT results ²	Rhodopsin level after light expose ³	LD ₅₀
A1 Hurricane Benzocaine	ethyl p-aminobenzoate 	Topical anesthetic, sore mouth and throat	125 3	1.5 (6)	50.0 (6)	X ⁴
A2 Flumadine Rimantadine	(RS)-1-(1-adamantyl)ethanamine 	Prophylaxis and treatment Influenza A virus	125 3	1.6 (6)	43.9 (6)	700

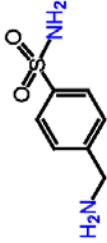
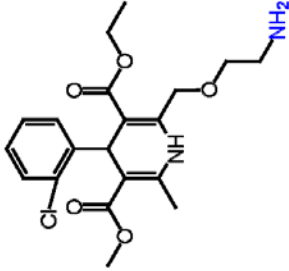
A3 Namenda Memantine hydrochloride	3,5-dimethyladamantan-1-amine 	Alzheimer's dementia	60 1.2	3.3 (6)	3.6 (5)	300
A4 Adipex-P Phentermine hydrochloride	2-methyl-1-phenylpropan-2-amine 	Weight reduction	14 0.3	1 (3)	77 (3)	x^4
A5 Pamate Tranylcypromine sulfate	(1R,2S)-2-phenylcyclopropan-1-amine 	Major depressive episodes	12 0.2	3 (3)	-0.04 (2)	205

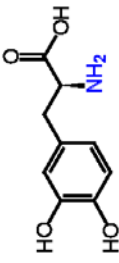
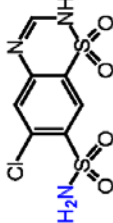

<p>A6</p> <p>Aminobenzoate potassium</p>	<p>2-aminobenzoic acid</p> 	<p>Scleroderma, fibrosis, dermatomyositis, nonsuppurative inflammation</p>	<p>400 8</p>	<p>2.7 (3)</p>	<p>2.2 (3)</p>	<p>2,000</p>
<p>A7</p> <p>Dapsone Aczone</p>	<p>4-[(4-aminobenzene)sulfonyl]aniline</p> 	<p>Dermatitis herpetiformis, leprosy</p>	<p>40 1</p>	<p>0.8 (3)</p>	<p>63.8 (3)</p>	<p>250</p>
<p>A8</p> <p>Paser Aminosalicylic Acid</p>	<p>4-amino-2-hydroxy-benzoic acid</p> 	<p>Tuberculosis</p>	<p>200 4</p>	<p>oral 1 (3) ip 1.5 (3)</p>	<p>67.1 (3) 51.6 (3)</p>	<p>2,800po 1,000ip</p>

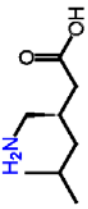
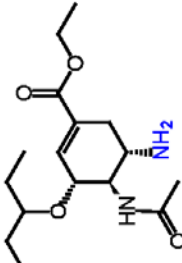
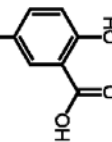
<p>A9 Luvox Fluvoxamine maleate</p>	<p>(E)-5-methoxy-1-[4-(trifluoromethyl)phenyl]pentan-1-one O-2-aminoethyl oxime</p> 	<p>Serotonin 5-HT reuptake inhibitor, social phobia, obsessive compulsive disorder</p>	<p>150 3.3</p>	<p>1.0 (3)</p>	<p>67.1 (3)</p>	<p>2,000</p>
<p>A10 Seromycin Cycloserine</p>	<p>(R)-4-amino-1,2-oxazolidin-3-one</p> 	<p>Antibiotic, pulmonary and extra pulmonary tuberculosis</p>	<p>800 20</p>	<p>1.7 (3)</p>	<p>66.9 (3)</p>	<p>5,290</p>

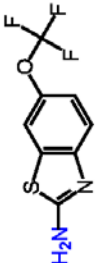
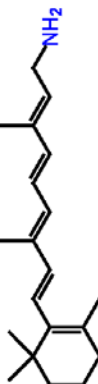
<p>A13R Januvia Janumet Sitagliptin</p>	<p>(R)-4-oxo-4-[3-(trifluoromethyl)-5,6-dihydro[1,2,4]triazolo[4,3-a]pyrazin-7(8H)-yl]-1-(2,4,5-trifluorophenyl)butan-2-amine</p> 	<p>Type 2 diabetes</p>	<p>15 0.34</p>	<p>1.3 (6)</p>	<p>66.7 (4)</p>	<p>200</p>
<p>A13S</p>	<p>(S)-4-oxo-4-[3-(trifluoromethyl)-5,6-dihydro[1,2,4]triazolo[4,3-a]pyrazin-7(8H)-yl]-1-(2,4,5-trifluorophenyl)butan-2-amine</p> 	<p>X⁴</p>	<p>15 0.34</p>	<p>2.2 (3)</p>	<p>38.6 (3)</p>	<p>X⁴</p>

<p>A14 Primaxin Cilastin Sodium</p>	<p>7-(2-amino-2-carboxy-ethyl) sulfonyl-2-(2,2-dimethylcyclopropyl) carbonylamino-hept-2-enoate</p>  <p>The structure shows a cyclopropyl ring attached to a carbonyl group, which is linked to a heptanoic acid chain. The heptanoic acid chain has a dimethylamino group at the 2-position and a sulfonamide group at the 7-position.</p>	<p>Potent antibacterial</p>	<p>250 6</p>	<p>3.3 (3)</p>	<p>18.6 (3)</p>	<p>1,489</p>
<p>A15 Prinivil Lisinopril</p>	<p>N²-[(1S)-1-carboxy-3-phenylpropyl]-L-lysyl-L-proline</p>  <p>The structure shows a proline ring connected to a lysine chain. The lysine chain has a 3-phenylpropyl group attached to the nitrogen atom and a carboxylic acid group at the end.</p>	<p>Hypertension, heart failure</p>	<p>400 8</p>	<p>3 (3)</p>	<p>41.5 (2)</p>	<p>2,000</p>

<p>A16 Sulfamylon Mafenide acetate</p>	<p>4-(aminomethyl)benzenesulfonamide</p>  <p>The structure shows a benzene ring with a sulfonamide group (-SO₂NH₂) at the para position and a methyleneamino group (-CH₂NH₂) at the other para position.</p>	<p>Antimicrobial, bacterial infection, burns, wounds</p>	<p>200 4</p>	<p>0.7 (3)</p>	<p>72.8 (3)</p>	<p>1,170</p>
<p>A17 Exforge Amlodipine</p>	<p>(RS)-3-ethyl 5-methyl 2-[(2-aminoethoxy)methyl]-4-(2-chlorophenyl)-6-methyl-1,4-dihydropyridine-3,5-dicarboxylate</p>  <p>The structure is a complex dihydropyridine derivative. It features a central dihydropyridine ring with an ethyl group at position 3, a methyl group at position 5, and a 2-aminoethoxy group at position 2. At positions 4 and 6, there are methyl and a 2-chlorophenyl group, respectively. The 3 and 5 positions are also substituted with methyl and ethyl groups, and the ring is part of a dicarboxylate salt.</p>	<p>Calcium channel blocker, hypertension</p>	<p>15 0.3</p>	<p>0.3 (3)</p>	<p>80.6 (3)</p>	<p>75</p>

<p>A18 Stalevo L-Dopa</p>	<p>(S)-2-amino-3-(3,4-dihydroxyphenyl) propanoic acid</p> 	<p>Parkinson's disease, crosses blood-brain barrier</p>	<p>450 10</p>	<p>3.7 (3)</p>	<p>-1.4 (3)</p>	<p>2,363</p>
<p>A19 Sodium Diuril Chlorothiazide sodium</p>	<p>6-chloro-1,1-dioxo-2H-1,2,4-benzothiazine-7-sulfonamide</p> 	<p>Diuretic, antihypertensive, edema in congestive heart failure, renal failure</p>	<p>2000 40</p>	<p>1.3 (3)</p>	<p>48.1 (3)</p>	<p>10,000</p>
<p>A20S Pregabalin</p>	<p>(S)-3-(aminomethyl)-5-methylhexanoic acid</p> 	<p>Neuropathic pain, post herpetic neuralgia, seizures, fibromyalgia</p>	<p>125 3</p>	<p>0.2 (3)</p>	<p>76.8 (3)</p>	<p>X⁴</p>

<p>A20R</p>	<p>(R)-3-(aminomethyl)-5-methylhexanoic acid</p> 	<p>X⁴</p>	<p>125 3</p>	<p>0.5 (3)</p>	<p>68.2 (3)</p>	<p>X⁴</p>
<p>A21 Tamiflu Oseltamivir phosphate</p>	<p>ethyl (3R,4R,5S)-5-amino-4-acetamido-3-(pentan-3-yloxy)cyclohex-1-ene-1-carboxylate</p> 	<p>Influenza infection and prophylaxis</p>	<p>180 3.3</p>	<p>3.7 (3)</p>	<p>-0.8 (3)</p>	<p>7,700</p>
<p>A22 Asacol Canasa Lialda Mesalazine/mesalamine</p>	<p>5-amino-2-hydroxybenzoic acid</p> 	<p>Ulcerative, rectal colitis, anti-inflammatory agent</p>	<p>125 2.6</p>	<p>oral 1.3 (3) ip 1.2 (6)</p>	<p>34.1 (3) 48.5 (6)</p>	<p>681</p>

<p>A23 Rilutek Riluzole</p>	<p>6-(trifluoromethoxy)benzothiazol-2-amine</p> 	<p>Amyotrophic lateral sclerosis</p>	<p>500 8</p>	<p>0.5 (3)</p>	<p>65.4 (3)</p>	<p>2,012</p>
<p>A24 Retinylamine</p>	<p>(2E,4E,6E)-3,7-dimethyl-9-(2,6,6-trimethylcyclohex-1-enyl)nona-2,4,6,8-tetraen-1-amine</p> 	<p>Experimental drug: inhibitor of retinoid isomerase</p>	<p>30 0.5</p>	<p>0.5 (6)</p>	<p>80.6 (6)</p>	<p>X⁴</p>

1- Short-term (acute) retinal degeneration was generated in *Abca4^{-/-}Rdh8^{-/-}* mice as described in Methods.

2- OCT results were calibrated as described in the manuscript. In short, 0 was assigned when no retinal degeneration was observed, 4, when the most severe retina degeneration was observed in untreated mice; n in parenthesis indicates the number of mice tested.

3- Levels of rhodopsin were deduced from measuring 11-cis-retinal in the eyes and results are shown as the percent of 11-cis-retinal remaining after illumination where 100% was the amount found in dark adapted mice unexposed to light (about 500 pmol/eye).

4- Unknown or not determined.

Supplementary Table 2. Distribution of SLO gray values after amine treatment of *Abca4*^{-/-}*Rdh8*^{-/-} mice for 3 months.

gray value ¹ dose (mg/mouse)	A20RS (2.0)	A20R (0.5)	A20R (2.0)	A22 (2.0)	Ret-NH ₂ (2.0)	vehicle -
0<10	2	0	0	0	0	0
10<20	6	1	6	0	8	0
20<30	4	10	5	8	1	2
30<40	2	2	3	3	1	6
40<50	1	1	1	3	0	5
50<60	0	0	0	1	0	6
60<	0	0	0	0	0	3
total numbers	15	15	15	15	10	22

¹*Abca4*^{-/-}*Rdh8*^{-/-} mice were treated daily by gavage with either A20RS (2 mg/mouse), A20R (0.5 or 2 mg/mouse) or A22 (2 mg/mouse) and weekly with A24 (2 mg/mouse) for 3 months beginning at 1 month of age (see **Fig. 6**, and **Supplementary Fig. 9**). The intensity of fundus autofluorescence in retinas of *Abca4*^{-/-}*Rdh8*^{-/-} mice was measured 3 months after treatment; autofluorescent SLO dial was set at 100 sensitivity. SLO mean gray values shown were calculated with Heidelberg's SLO software. The intensity of autofluorescence in retinas of amine-treated *Abca4*^{-/-}*Rdh8*^{-/-} mice was significantly less than that of vehicle-treated animals.